

# Impact of removal frequency on site-specific force profile and dimensional stability of direct-printed aligners in relation to dental crowding: an in vitro comparative study

**Nurdana Darkhanbayeva**

Kyung Hee University College of Dentistry, Kyung Hee University Dental Hospital

**Jin-Young Choi**

Kyung Hee University College of Dentistry, Kyung Hee University Dental Hospital

**Kun Woo Park**

Kyung Hee University College of Dentistry, Kyung Hee University Dental Hospital

**Hwarang Jeong**

Kyung Hee University College of Dentistry, Kyung Hee University Dental Hospital

**Hoon Kim**

Graphy Inc

**Jung-Yul Cha**

Yonsei University College of Dentistry

**Su-Jung Kim**

ks.j113@khu.ac.kr

Kyung Hee University College of Dentistry, Kyung Hee University Dental Hospital



---

## Research Article

**Keywords:** direct-printed aligner, thermoformed aligner, force decay, dimensional stability, dental crowding

**Posted Date:** April 14th, 2025

**DOI:** <https://doi.org/10.21203/rs.3.rs-6259817/v1>

**License:**   This work is licensed under a Creative Commons Attribution 4.0 International License. [Read Full License](#)

**Additional Declarations:** No competing interests reported.

---

# Abstract

## Background

This *in vitro* comparative study examined the effects of high removal frequency on force generation and gap width changes in direct-printed aligners (DPAs) compared with thermoformed aligners (TFAs), considering different tooth positions and crowding conditions.

## Methods

A total of 104 aligners, comprising 26 pairs of DPAs and 26 pairs of TFAs, were fabricated for both crowded and noncrowded maxillary arch models. Force measurements were conducted at initial placement and after every 20 removal cycles for up to 100 cycles, whereas gap width analyses were performed at initial placement and after 100 removal cycles. Statistical analyses were performed to evaluate the force and gap width changes, with a focus on site-specific differences.

## Results

DPAs demonstrated significantly lower initial forces and maintained consistent force levels over increased removal frequencies, irrespective of crowding conditions. Conversely, TFAs exhibited higher initial forces, with significant force decay over time, particularly in crowded models. DPAs also showed improved fit over time with decreased gap widths, whereas the gap widths of TFAs increased, particularly in the gingival areas.

## Conclusion

DPAs offer superior dimensional stability and force predictability over TFAs while maintaining consistent performance across various dental conditions. Future *in vivo* studies are recommended to further explore the clinical efficacy of DPA and address its current limitations.

## BACKGROUND

The advent of clear aligners (CAs) has revolutionized orthodontic treatment by offering an aesthetic, comfortable, hygienic, and convenient alternative to fixed appliances [1], which are highly preferred by patients [2, 3]. Moreover, advances in materials and manufacturing methods have significantly enhanced the clinical performance of CAs, thereby expanding their applicability to various types of malocclusions [4–6]. The integration of digital technology with three-dimensional (3D) printing has minimized labor-intensive fabrication and reduced cumulative processing errors associated with traditional thermoplastic workflows [7]. Direct-printed aligners (DPAs), which bypass the intermediary step of 3D model printing, utilize innovative materials, such as photopolymerizable polyurethane (Tera Harz TC-85 DAC UV Resin; Graphy Inc., Seoul, Korea). This advancement enables same-day appliance delivery via in-house fabrication. DPAs are expected to deliver more consistent and predictable orthodontic forces than thermoformed aligners (TFAs) owing to their shape memory properties and dimensional stability at high temperatures [8].

To achieve planned tooth movements, CAs must exert controlled forces on target teeth with minimal unintended force fluctuation decay. Understanding the mechanical properties of a material that affects the biomechanical behavior of the appliance is crucial. However, evidence is limited because of the complexity of analyzing the entire arch force system exerted by CAs. Studies have explored various mechanical properties of DPAs, including their thermomechanical characteristics, viscoelasticity, stress relaxation and creep, shape recovery, ultraviolet (UV) curing kinetics, and cytotoxicity [9–16]. Ensuring the dimensional accuracy of DPAs is critical for optimal fit and stability throughout the treatment period. Any discrepancy in fit may lead to insufficient physiological activation of alveolar remodeling or excessive force on the teeth, complicating the force system and making it unpredictable. Therefore, maintaining close contact between the aligner and tooth surfaces is essential despite repeated mechanical stresses over time [17]. Notably, manufacturers recommend a minimum gap width of 50  $\mu\text{m}$  for fabrication purposes. This raises questions regarding whether DPAs fit the reference model better than TFAs prior to activation in the mouth.

Previous studies compared the dimensional accuracies of DPAs and TFAs under various conditions and yielded mixed results. Studies using metrology software for alignment have shown that DPAs fit more accurately than TFAs, suggesting that DPAs deliver more aligned forces with biologically desired levels and biomechanically consistent profiles [11, 18]. Conversely, based on site-specific morphometric analyses, a recent micro-computed tomography (CT) study found greater gap widths in DPAs than in TFAs, particularly in the palatal, buccogingival, and palatogingival regions, based on site-specific morphometric analyses [19]. Moreover, dimensional stability after repeated aligner deflection due to frequent insertion and removal is vital for consistent force delivery. Although studies have shown decreased forces in TFAs with increased removal frequency [20], similar investigations on DPAs are lacking. An *in vivo* study on DPAs [8] indicated no significant changes in the mechanical properties after 1 week of intraoral aging, although the sample size was limited.

Predicting the force levels delivered to each tooth remains challenging because tooth movement with CAs is not solely dependent on the shape-molding effect. Various factors influencing the loading force changes have been identified, including material properties, degradation over time, removal frequency, tooth irregularity, and inbuilt activation [20]. However, it is crucial to minimize the discrepancies between the intimate contact areas and relief areas within activated aligners [21]. Before assessing the viscoelastic properties, it is important to verify the effect of the aligner removal frequency on non-activated aligners by correlating force changes with gap width alterations due to deformation.

This *in vitro* study aimed to investigate the site-specific effects of removal frequency on the dimensional stability and consequent loading force changes in DPAs compared with TFAs, focusing on the central incisor, canine, second premolar, and second molar regions within a crowded dental arch. The null hypothesis posited that DPAs would exhibit no significant changes in gap width and force levels across all tooth surfaces after repeated appliance removal, regardless of tooth position or anterior crowding.

## METHODS

### Sample Preparation

A master scan of the maxillary arch with well-aligned occlusion after orthodontic treatment was obtained using an intraoral scanner (Trios, 3shape, Copenhagen, Denmark) for control purposes. The standard tessellation language (STL) file was imported into the Autolign software (Diorco Co., Ltd., Seoul, Korea) to create another STL file of the maxillary arch with a tooth-size-arch-length discrepancy of 6 mm for the study sample. Two types of digital master models were produced: one with crowding (C) and one without crowding (NC). Ten master models were printed for each group using a digital light processing (DLP) 3D printer (Asiga UV MAX385, Asiga, Alexandria, Australia) at a 50- $\mu$ m layer thickness. A total of 104 aligners were fabricated: 26 pairs of DPAs (DPA\_C and DPA\_NC) and 26 pairs of TFAs (TFA\_C and TFA\_NC) for both the C and NC groups (Fig. 1). In each aligner group, 20 pairs were used for the film-sensor tests and 6 pairs were used for micro-CT analysis. The sample size per group was estimated to be 16, as determined using the G\* Power software (version 3.1.9.7, Düsseldorf, Germany), according to previous studies [20]. An effect size of 0.4, a power of 90%, and an  $\alpha$  value of 0.05 were applied.

## DPA Fabrication

DPAs were digitally designed using Deltaface software (Coruo, Limoges, France) with a predetermined thickness of 0.50 mm and an offset of 50  $\mu$ m. The aligner margins on the facial sides were digitally trimmed to approximately 1 mm below the gingival margins, following the natural contour. They were positioned at a printing angle of 30° for minimal support struts and printed using a TC-85DAC 3D Printing Shape Memory Aligner Resin (Graphy Inc., Seoul, Korea) and a DLP 3D printer (Asiga UV MAX385, Asiga, Alexandria, Australia). The residual resin was removed from the printed aligners by using a centrifuge (Tera Harz Spinner, Graphy Inc., Seoul, Korea) at 500 rpm for 5 min. The DPAs were then cured for 20 min with UV light (405 nm) under nitrogen atmosphere using a post-curing machine (Tera Harz Cure, Graphy Inc., Seoul, Korea). The final cleaning was performed using an ultrasonic cleaner for 2 min at 80°C.

## TFA Fabrication

A 0.75-mm thickness of polyethylene terephthalate glycol (PET-G) sheet, branded as Easy-Vac gasket (3A MEDES, Korea), was utilized to vacuum-thermoform the passive aligner over the printed master models using a pressurized thermoforming machine (Biostar, Scheu-Dental, Iserlohn, Germany), following the manufacturer's recommendations. The thermoformed sheet was removed from the model and trimmed along the same gingival edges as the DPA. All TFAs ( $n = 52$ ) were produced by a single technical expert (N. D.) using the same master model of the TFA\_C or TFA\_NC samples.

## Force Measurement

A thin-film single pressure sensor (FlexiForce ESS102, Tekscan Inc. USA) was used to measure the compression exerted by the aligners on each tooth surface (Fig. 2a). The sensors, featuring soft and flexible structures with minimal thickness (0.203 mm), a small sensing area (3.8-mm diameter), high sensitivity, and a measurable force range of 4.4 N (448.668 g), were employed. During the final step of fabrication of the printed master model for force measurement, the facial surfaces of the relevant teeth were specially designed to provide a perfectly fit space for sensor installation. To minimize the sensor weight imbalance due to the

discrepancy between the flat sensor and curved inner aligner surface, the sensors were trimmed, and tooth surfaces were optimally prepared to enhance sensor performance (Fig. 2b). Four sensors were fixed to the prefabricated facial surfaces of the central incisor (#11), canine (#13), second premolar (#15), and second molar (#17) of each master model using cyanoacrylate (Fig. 2c). All sensors were reset and calibrated across different model-sensor-aligner complexes before measurement to ensure consistent loading geometry and environmental conditions. Ten samples were randomly selected for reproducibility testing by precision rate [20], and the averaged precision rate between repeated measurements was found to be  $93.2 \pm 2.8\%$ .

Force measurements were conducted at the initial placement of the aligner (T0), after every 20 removals (T20, T40, T60, and T80), and after removal up to 100 times (T100). The process of placing and removing aligners was performed exactly as orthodontists recommend to patients, according to the aligner type. For DPAs, repeated insertion and removal were conducted inside a water bath at 45°C, and force was measured in a laboratory oven set at 37°C after a 1-h stay to fully express its shape memory property (Fig. 2d). For TFAs, all procedures were performed at room temperature. The entire process was performed by a single technician (N. D.). Sensor data collection was conducted using the ELF system software (Tekscan, Inc. USA) (Fig. 2e and 2f).

## Gap Width Measurement

All aligners over the corresponding master models in the TFA\_C, TFA\_NC, DPA\_C, and DPA\_NC groups (n = 6 each) were scanned at T0 and T100 using a high-resolution micro-CT (Skyscan1173, Bruker, MA, USA) at 40 kV, 200 µA, and 35-µm resolution. The resulting 3D images (n = 48) of each target tooth were reoriented using the DataViewer software (version 1.5.6.2, Bruker, MA, USA). Midsagittal longitudinal slices perpendicular to both the model base plane and the line linking the most mesial and distal contact points were obtained for the central incisors and canines (Fig. 3a). Longitudinal slices were constructed for the premolars and molars that passed through the facial and palatal cusp points (FC and PC, respectively) (Fig. 3b). Gap widths were measured using the CTAn software (release 2.5, Bruker, MA, USA) at 300x magnification as the shortest distance when a perpendicular line was projected from each reference point tangent on the tooth. The reference points included gingival margins, facial and palatal contour heights, incisal edge/cusp points, and the most concave cingulum/occlusal pit: facial (F); faciogingival (FG); palatal (P); palatogingival (PG); and additionally, incisal (IN) for anterior teeth; FC, PC, and occlusal fossa (OF) for posterior teeth.

## Statistical Analysis

We performed inter-group comparisons of forces at different aligner removal frequencies between DPAs and TFAs according to tooth position and presence of crowding. In addition, the gap width differences between the model and aligner after 100 removal cycles and the DPAs and TFAs across various tooth regions in both the C and NC groups were compared.

This was confirmed using a linear mixed-effects model for repeated data, and the interaction effects between the removal point, appliance, and crowding were evaluated through the interaction term. Additionally, multiple comparisons using Bonferroni post-hoc correction were carried out.

All statistical analyses were performed based on a significance level of 0.05, and SAS9.4 (SAS Institute, Inc., Cary, NC) and R4.4.2 (<https://cran.r-project.org>) were used for statistical analyses.

## RESULTS

### Comparison of the Force Levels Between Aligners at Different Removal Frequencies

At the initial placement (T0), DPA exerted significantly lower forces than TFA did in the C and NC groups across all tested teeth (Table 1). The forces delivered by TFA were notably lower in the C group ( $20.81 \pm 10.94$  g to  $79.15 \pm 18.35$  g) compared with the NC group ( $132.75 \pm 46.19$  g to  $181.64 \pm 46.36$  g) at all tested frequencies up to T100, except for the second molars. In contrast, the forces exerted by DPA showed no differences between the groups based on crowding or tooth position and remained within a narrow range ( $4.68 \pm 1.23$  g to  $7.58 \pm 0.70$  g).

Table 1

Inter-group comparisons of forces at different aligner removal frequencies between DPA and TFA, categorized by tooth position and the presence of crowding (values in parentheses represent the relative ratio when T0 is considered as 100).

Tooth #	Removal Frequency	DPA Group		TFA Group		P-value of Interaction
		DPA_NC	DPA_C	TFA_NC	TFA_C	
#11	T0	7.47 ± 0.63	6.07 ± 0.75	181.03 ± 43.51	33.20 ± 10.67	
	T20	7.56 ± 0.78	6.13 ± 0.79	169.93 ± 41.60	29.76 ± 10.71	0.328
	T40	7.32 ± 0.73	6.16 ± 0.79	166.60 ± 41.78	29.17 ± 10.97	0.09
	T60	7.55 ± 0.78	6.20 ± 0.67	161.35 ± 38.40	24.85 ± 10.62	< .001 <sup>***</sup>
	T80	7.48 ± 0.55	6.17 ± 0.63	156.03 ± 37.72	23.41 ± 10.43	< .001 <sup>***</sup>
	T100	7.58 ± 0.70	6.11 ± 0.81	148.51 ± 39.41	20.81 ± 10.94	< .001 <sup>***</sup>
	P-value <sup>†</sup>	0.285	0.378	<.001 <sup>†††</sup>	<.001 <sup>†††</sup>	< .001 <sup>***</sup>
	P-value <sup>‡</sup>	0.916		<.001 <sup>†††</sup>		
#13	T0	4.74 ± 1.23	5.34 ± 0.98	173.74 ± 44.53	79.15 ± 18.35	
	T20	4.71 ± 1.28	5.37 ± 0.84	159.34 ± 42.92	68.82 ± 19.28	0.162
	T40	4.83 ± 1.33	5.36 ± 0.96	154.70 ± 44.24	65.08 ± 18.50	0.261
	T60	4.68 ± 1.23	5.60 ± 1.12	150.06 ± 42.54	61.70 ± 16.75	0.008 <sup>**</sup>
	T80	4.70 ± 1.15	5.43 ± 0.83	145.67 ± 40.67	56.16 ± 16.50	0.003 <sup>**</sup>
	T100	4.83 ± 1.20	5.41 ± 0.80	137.63 ± 40.91	53.15 ± 15.61	0.032 <sup>*</sup>
	P-value <sup>†</sup>	0.247	0.073	<.001 <sup>†††</sup>	<.001 <sup>†††</sup>	0.005 <sup>**</sup>

<sup>†</sup>Analysed by liner mixed-effects model for repeated measures. <sup>†</sup>, P < 0.05; <sup>††</sup>, P < 0.01; <sup>†††</sup>, P < 0.001.

<sup>‡</sup>Analysed linear mixed-effects model with interaction terms for removal frequency and appliance. <sup>‡</sup>, P < 0.05; <sup>‡‡</sup>, P < 0.01; <sup>‡‡‡</sup>, P < 0.001.

<sup>\*</sup>Analysed linear mixed-effects model with interaction terms for removal frequency, appliance, and crowding presence. <sup>\*</sup>, P < 0.05; <sup>\*\*</sup>, P < 0.01; <sup>\*\*\*</sup>, P < 0.001.

	<b>P-value<sup>‡</sup></b>	0.865		<.001 <sup>##</sup>		
#15	<b>T0</b>	5.95 ± 0.80	6.06 ± 0.66	181.64 ± 46.36	56.50 ± 15.67	
	<b>T20</b>	6.20 ± 0.97	6.20 ± 0.66	164.69 ± 42.62	48.36 ± 16.20	0.586
	<b>T40</b>	6.02 ± 0.87	6.21 ± 0.54	152.76 ± 42.07	46.84 ± 14.72	0.646
	<b>T60</b>	5.87 ± 0.86	6.24 ± 0.52	147.40 ± 44.85	41.69 ± 13.54	0.057
	<b>T80</b>	5.79 ± 0.95	6.10 ± 0.58	143.68 ± 42.84	38.70 ± 11.66	0.02*
	<b>T100</b>	5.94 ± 0.86	6.01 ± 0.68	132.75 ± 46.19	34.99 ± 9.09	0.135
	<b>P-value<sup>†</sup></b>	0.098	0.319	<.001 <sup>†††</sup>	<.001 <sup>†††</sup>	0.017*
	<b>P-value<sup>‡</sup></b>	0.373		0.015 <sup>‡</sup>		
#17	<b>T0</b>	5.07 ± 0.35	5.04 ± 0.44	162.66 ± 44.27	167.07 ± 42.23	
	<b>T20</b>	5.17 ± 0.55	5.16 ± 0.41	144.56 ± 44.97	152.85 ± 36.24	0.573
	<b>T40</b>	5.08 ± 0.48	5.17 ± 0.34	136.76 ± 42.73	145.29 ± 37.16	0.855
	<b>T60</b>	5.20 ± 0.53	5.15 ± 0.36	126.49 ± 39.43	136.95 ± 39.04	0.423
	<b>T80</b>	5.08 ± 0.41	5.22 ± 0.46	117.65 ± 38.24	128.85 ± 36.53	0.76
	<b>T100</b>	5.18 ± 0.38	5.10 ± 0.31	104.12 ± 37.89	118.92 ± 35.77	0.107
	<b>P-value<sup>†</sup></b>	0.423	0.221	<.001 <sup>†††</sup>	<.001 <sup>†††</sup>	0.177
	<b>P-value<sup>‡</sup></b>	0.934		0.085		
<sup>†</sup> Analysed by liner mixed-effects model for repeated measures. <sup>†</sup> , P < 0.05; <sup>††</sup> , P < 0.01; <sup>†††</sup> , P < 0.001.						
<sup>‡</sup> Analysed linear mixed-effects model with interaction terms for removal frequency and appliance. <sup>‡</sup> , P < 0.05; <sup>##</sup> , P < 0.01; <sup>###</sup> , P < 0.001.						
<sup>*</sup> Analysed linear mixed-effects model with interaction terms for removal frequency, appliance, and crowding presence. <sup>*</sup> , P < 0.05; <sup>**</sup> , P < 0.01; <sup>***</sup> , P < 0.001.						

## Comparison of Force Changes Between Aligners: Effects of Crowding and Tooth Position



The linear mixed-effects model for repeated measures indicated that the forces exerted by TFA significantly decreased with increasing removal frequency in the NC and C groups. However, the forces exerted by DPA showed no significant changes over time in either group (NC or C). Regarding the relative force rate at each removal frequency, the greatest reduction was observed in the TFA\_C group, followed by the TFA\_NC group, whereas the DPA\_C and DPA\_NC groups maintained consistent force levels across all removal frequencies. This trend was most pronounced in the central incisors, where the relative force levels were 61.05%, 81.69%, 101.53%, and 100.64% in the TFA\_C, TFA\_NC, DPA\_NC, and DPA\_C groups, respectively. A linear mixed-effects model with interaction terms revealed significant effects of crowding on the force levels for the central incisors, canines, and second premolars in the TFA samples only. For the second molars, the relative force levels in the TFA samples showed no differences based on the presence of crowding (Table 1 and Fig. 4).

## **Comparison of Gap Widths Between Aligners at Different Tooth Surface Areas**

The initial gap widths (T0) exhibited site-specific differences across all tooth surfaces between DPA and TFA depending on the tooth position (Table 2). In both NC and C groups, TFA exhibited the greatest gap at the PG and OF areas for anterior ( $173.57 \pm 32.36 \mu\text{m}$  to  $298.03 \pm 41.74 \mu\text{m}$ ) and posterior teeth ( $140.71 \pm 16.97 \mu\text{m}$  to  $316.26 \pm 58.83 \mu\text{m}$ ), respectively, and the smallest gaps at the F surfaces for the anterior teeth ( $4.06 \pm 6.23 \mu\text{m}$  to  $36.79 \pm 24.02 \mu\text{m}$ ), indicating a large variation in gap width depending on the location. In contrast, DPA displayed the largest gaps at the IN area for anterior teeth ( $85.95 \pm 19.61 \mu\text{m}$  to  $117.10 \pm 26.72 \mu\text{m}$ ) and at the FG and PG areas for posterior teeth ( $139.93 \pm 23.93 \mu\text{m}$  to  $232.66 \pm 32.58 \mu\text{m}$ ), showing relatively uniform gap distribution.

Table 2  
Initial (T0) and after 100 removal frequencies (T100) micro-CT gap widths at each region of interest, categorized by tooth position and the presence of crowding, for two types of aligners.

Tooth #	Surface Area	T0	T100						
		DPA_NC	TFA_NC	DPA_C	TFA_C	DPA_NC	TFA_NC	DPA_C	TFA_C
#11	PG	98.87 ± 8.43	228.01 ± 32.07	86.23 ± 16.84	298.03 ± 41.74	94.80 ± 8.39	243.59 ± 39.57	80.42 ± 14.86	303.59 ± 43.08
	P	88.93 ± 12.58	113.08 ± 27.60	92.94 ± 10.87	236.42 ± 78.52	87.26 ± 10.11	108.14 ± 26.43	86.08 ± 7.87	235.03 ± 76.73
	IN	147.11 ± 26.72	54.08 ± 8.57	141.52 ± 9.52	111.34 ± 39.25	146.59 ± 29.24	53.00 ± 9.24	131.98 ± 8.30	110.86 ± 36.88
	F	49.09 ± 3.11	4.06 ± 6.23	58.10 ± 7.85	30.61 ± 6.31	50.36 ± 2.61	3.53 ± 4.51	53.04 ± 4.15	30.60 ± 5.83
	FG	142.35 ± 37.05	97.42 ± 21.06	115.96 ± 13.65	136.34 ± 27.24	138.73 ± 36.22	104.93 ± 18.06	110.07 ± 9.22	141.21 ± 26.08
	P-value <sup>†</sup>	<.001 <sup>+++</sup>			<.001 <sup>+++</sup>				
#13	PG	89.14 ± 11.64	173.57 ± 32.36	96.39 ± 9.15	194.22 ± 121.48	87.64 ± 13.24	178.43 ± 32.60	93.70 ± 5.97	200.13 ± 123.45
	P	74.53 ± 11.81	77.63 ± 11.99	60.99 ± 11.46	93.34 ± 53.08	72.67 ± 11.24	77.15 ± 11.80	55.03 ± 13.95	93.34 ± 53.08
	IN	117.97 ± 18.34	65.88 ± 12.34	85.95 ± 19.60	151.32 ± 151.88	117.62 ± 20.31	64.62 ± 11.06	86.72 ± 16.88	146.54 ± 142.94
	F	62.73 ± 13.04	6.71 ± 4.40	99.56 ± 18.83	36.79 ± 24.02	62.78 ± 9.37	3.75 ± 2.06	98.65 ± 18.22	36.06 ± 28.65
	FG	89.09 ± 19.36	80.41 ± 13.84	135.60 ± 30.13	187.21 ± 66.32	86.98 ± 23.29	79.21 ± 10.93	135.84 ± 33.04	190.63 ± 62.62
	P-value <sup>†</sup>	0.218			0.218				
#15	PG	255.56 ± 25.49	304.54 ± 39.34	213.01 ± 59.11	316.26 ± 58.83	254.11 ± 24.03	318.20 ± 48.51	196.14 ± 47.64	324.62 ± 59.87
	P	65.88 ± 12.34	54.00 ± 8.57	79.24 ± 7.86	121.48 ± 21.05	64.52 ± 10.99	53.39 ± 7.88	80.16 ± 6.46	125.48 ± 17.37
	PC	125.57 ± 13.24	70.00 ± 9.44	118.41 ± 19.27	97.42 ± 16.84	124.34 ± 13.22	65.95 ± 6.70	110.18 ± 21.46	98.28 ± 14.42
	OF	105.12 ± 19.12	564.04 ± 50.12	112.53 ± 12.60	458.46 ± 72.94	102.57 ± 20.84	564.27 ± 49.02	112.13 ± 12.58	454.79 ± 72.49
<sup>†</sup> Analysed linear mixed-effects model with interaction terms for surface point, appliance, and crowding presence. <sup>†</sup> , P < 0.05; <sup>††</sup> , P < 0.01; <sup>†††</sup> , P < 0.001.									

	<b>FC</b>	132.17 ± 17.30	42.46 ± 6.53	149.48 ± 71.35	49.00 ± 15.94	130.41 ± 14.27	41.49 ± 6.39	124.70 ± 52.71	49.08 ± 15.38
	<b>F</b>	86.07 ± 13.27	33.78 ± 2.34	99.96 ± 12.40	33.47 ± 2.41	85.59 ± 12.72	32.82 ± 2.77	104.57 ± 15.39	34.22 ± 2.35
	<b>FG</b>	230.47 ± 38.27	99.40 ± 15.88	232.67 ± 32.58	97.19 ± 45.11	222.45 ± 29.17	99.82 ± 15.69	242.63 ± 28.22	102.93 ± 45.23
	<b>P-value †</b>	0.006 <sup>††</sup>				0.006 <sup>††</sup>			
#17	<b>PG</b>	123.26 ± 15.14	140.71 ± 16.97	134.00 ± 35.49	281.75 ± 79.05	122.53 ± 13.18	147.39 ± 20.16	132.90 ± 32.44	285.27 ± 76.58
	<b>P</b>	68.52 ± 16.81	72.15 ± 4.16	70.34 ± 10.34	77.48 ± 17.50	69.52 ± 12.91	71.01 ± 3.49	67.80 ± 8.47	80.32 ± 16.98
	<b>PC</b>	104.31 ± 15.31	78.93 ± 10.09	120.67 ± 26.36	68.27 ± 14.76	103.45 ± 14.74	77.05 ± 9.56	115.96 ± 26.03	66.92 ± 13.53
	<b>OF</b>	94.00 ± 3.66	393.70 ± 49.89	78.55 ± 9.80	268.74 ± 73.09	92.71 ± 4.63	402.28 ± 49.74	76.24 ± 11.72	267.89 ± 70.95
	<b>FC</b>	106.95 ± 14.36	125.51 ± 11.49	124.59 ± 17.43	98.39 ± 19.31	105.75 ± 14.07	127.27 ± 12.66	117.80 ± 17.30	101.28 ± 18.64
	<b>F</b>	94.68 ± 13.65	98.18 ± 7.06	60.98 ± 12.02	55.05 ± 16.81	92.16 ± 13.75	101.06 ± 8.10	62.39 ± 13.84	57.03 ± 16.41
	<b>FG</b>	139.93 ± 23.93	84.47 ± 14.43	143.67 ± 31.27	72.18 ± 11.39	139.08 ± 23.59	88.89 ± 14.39	141.53 ± 31.10	74.37 ± 11.08
	<b>P-value †</b>	0.035 <sup>†</sup>				0.035 <sup>†</sup>			
†Analysed linear mixed-effects model with interaction terms for surface point, appliance, and crowding presence. †, P < 0.05; ††, P < 0.01; †††, P < 0.001.									

## Comparison of Gap Width Changes Between Aligners: Effects of Crowding and Tooth Position

After 100 removal cycles, TFA showed significant increases in gap widths at the gingival margin areas (PG and FG) in the NC group. In contrast, the DPA\_NC group exhibited significant decreases in the gap width at the FG and PG areas of the central incisors and the F area of the second molar, with no gap width changes observed at other tooth areas. In the C group, the change in gap width in the TFA\_C group was reduced compared to the TFA\_NC group, whereas the decrease in gap width in the DPA\_C group was greater than that in the DPA\_NC group. Notably, for the rearmost teeth (#17), neither aligners demonstrated significant gap width changes in the presence of crowding, except at the FC area in the DPA group. Linear mixed model analysis further revealed that, for DPA, crowding had a minimal impact on gap width changes, whereas for TFA, crowding significantly influenced the extent of gap width changes across different tooth regions, particularly for tooth #15. Interestingly, for tooth #15, the difference in the gap width changes between the PG and other regions was greater in the absence of crowding than when crowding was present in the TFA group.

In the DPA group, particularly in the presence of crowding, the variance in the gap width differences between regions was large. However, owing to the small sample size and high standard deviation (SD), the statistical significance of these differences could not be determined (Fig. 5).

## DISCUSSION

This *in vitro* comparative study examined the impact of high removal frequency on force generation and gap width changes in DPA compared with TFA, considering different tooth positions and crowding conditions. The significance of this study lies in its potential to provide a foundational guideline for understanding how forces are applied when using DPA to effectively deliver planned forces across all teeth. Compared with TFAs, DPAs produced from each step of the digital master model consistently demonstrated more uniform fit across different teeth and positions from the first insertion, regardless of the degree of crowding. This lower discrepancy may ensure that the orthodontic forces are exerted relatively uniformly and as digitally planned.

This study primarily assessed the initial forces applied by each aligner to facial tooth surfaces in the same master model, correlating with site-specific aligner fit differences. Theoretically, TFA should exert no significant initial force on the master model to deliver purely programmed forces intraorally. However, the initial forces from TFA were high, exceeding 100 g, when the sensor resistance and sensitivity were set to detect the minimal positive force from DPA (4–8 g). TFA exerted the greatest force on the central incisors and the least on the second molars, likely due to substantial gap discrepancies between the F and P surfaces of the incisors (Gap\_F, 4.06  $\mu\text{m}$ ; Gap\_P, 113.08  $\mu\text{m}$ ; Gap\_PG, 228.01  $\mu\text{m}$  in the TFA\_NC group, and Gap\_F, 30.61  $\mu\text{m}$ ; Gap\_P, 236.42  $\mu\text{m}$ ; Gap\_PG, 298.03  $\mu\text{m}$  in the TFA\_C group). This uneven aligner fit could push the incisors palatally, potentially offsetting programmed forces, and leading to unexpected or insufficient movement with TFA. In contrast, DPA exerted low initial forces (< 7.5 g), aligning with more even gap width distribution across the tested teeth (51.09  $\mu\text{m}$  to 98.87  $\mu\text{m}$  in the DPA\_NC group and 60.10  $\mu\text{m}$  to 92.94  $\mu\text{m}$  in the DPA\_C group), corroborating previous findings using digital best-fit alignment algorithms [19].

Furthermore, DPA maintained lower forces steadily over increased removal frequencies, demonstrating significant dimensional stability over time, whereas the forces exerted by TFA gradually decreased, as reported in previous studies [20, 22]. Lombardo et al. [23] demonstrated that thermoformed materials exhibit substantial initial stress, followed by notable stress relaxation and yield stress changes, leading to significant force loss over time. Our micro-CT findings confirmed permanent TFA deformation, particularly at the gingival margins, which contributed to force loss. In the TFA\_NC group, force decay was greatest in the second molars (36.28%), followed by the second premolars (27.42%), canines (21.25%), and central incisors (18.31%). In contrast, in the TFA\_C group, force decay occurred in the order of the central incisors (38.95%), second premolars (36.56%), canines (33.16%), and second molars (28.41%), indicating that in cases with crowding, the reduction in force with removal frequency was more pronounced. The aligner removal frequency did not affect the force profile of DPA, which was supported by the significant dimensional stability across most of the tested surfaces. Interestingly, the initial DPA gaps in the gingival margins were decreased by T100 in the central incisors and second premolars, improving the overall fit. In contrast, TFA exhibited an increase in gingival margin gaps by T100 in the central incisors, second premolars, and second molars, indicating that changes in the gingival margin area were the most significant differences. Consequently, DPA is likely to

deliver more predictable orthodontic forces as programmed, even after 100 removal cycles, with no significant differences in the overall gap and with improved fit.

A key aspect of this study was the examination of the impact of crowding on force profiles and dimensional stability. The low and constant initial loading forces of DPA remained unaffected by moderate tooth irregularity, showing no crowding-dependent gap width differences. This contrasts with TFA, where crowding led to significant initial force reductions and increased gap widths around overlapping teeth. Specifically, the P surfaces of the central incisors and canines showed increased gaps due to lingually blocked lateral incisors, reducing the undesired initial forces observed in the TFA\_NC group. However, this may limit the alignment efficiency in the target movement areas, highlighting design considerations. Notably, compared to the noncrowded models, the crowded models exhibited a greater TFA force decay, especially in the central incisors, while there were no significant differences observed in the second molars. Thus, the performance of TFA may be highly susceptible to intraoral conditions, such as crowding and tooth position, leading to unpredictable outcomes. Fiori et al. [24] found clinical challenges in achieving predictable movement with TFA in crowded conditions, particularly in the facial movement of the maxillary canines and first premolars. In our study, crowding was found to significantly affect gap width variation, especially in the premolar regions, suggesting that such irregular and unpredictable changes may contribute to the inefficient movement of the premolars with TFA. However, due to the design of our study, the greater gap width changes observed near the gingival area did not perfectly align with the force changes measured at the center of the crown. Consequently, owing to the geometric accuracy and reduced site-specific differences, DPA may ensure passive-fit adaptation in crowded dentition, facilitating a more predictable alignment.

The effect of the removal frequency on the gap width variation further underscores the differences between DPA and TFA. Interestingly, DPA maintained a fairly constant gap width after repeated deformations, even in the presence of tooth crowding. This stability can be attributed to the viscoelastic properties of the material of DPA. Lee et al. [9] demonstrated that the stress relaxation and creep behavior of TC-85 showed less stress release at 80°C compared with 37°C while maintaining static force after 13 loading cycles. The elastic modulus and elasticity of TC-85 arise from temperature-dependent changes in the attractive forces between the polymer chains, indicating that soaking DPA in hot water can enhance its initial tooth adaptation, particularly in crowded dentitions. Furthermore, TC-85 is highly durable owing to its interconnected structure, which allows it to retain its shape after repeated exposure.

In contrast, TFA lacks shape memory properties because it is composed of a thermoplastic polymer. When deformed in the permanent deformation region, thermoplastic polymers cannot return to their original shape. Additionally, although most polymer tests are conducted at 25°C, the oral environment typically has a temperature of approximately 37°C. This higher temperature transfers energy to the polymer molecules, causing them to easily lose their original shape. Conversely, the 3D network molecular structure of DPA allows it to maintain its original shape and mechanical properties even at elevated temperatures. This inherent stability ensures a consistent and reliable mechanical performance.

During the experimental process, DPA showed an improved fit to the model with repeated insertions and removals, whereas TFA exhibited a decreased fit under the same conditions. This phenomenon can be explained based on the material properties of each aligner. TFA is a thermoplastic polymer that undergoes

deformation and lacks the ability to revert to its original shape. In contrast, DPA is composed of a UV-curable polyurethane acrylate-based polymer with a 3D network structure.

More importantly, the increased fit of DPA after repeated insertions and removals can be attributed to the reorganization of unstable urethane bonds. During 3D printing, urethane acrylate oligomers in DPA become fixed in a random and sterically hindered state. However, through repeated cycles of deformation and recovery, the unstable urethane bonds gradually reorganize into a more stable configuration. This process enhances the recovery force of the deformed polymer, resulting in an improved fit and better mechanical performance over time.

Our findings of improved fit of DPA over time suggest its clinical advantages over TFA in adapting to tooth position-aligned mismatches when delivered intraorally. Linjawi et al. [25] suggested wearing Invisalign for 15 days for the best aligner fit, in terms of minimum gap width, using scanning electron microscopy. The dimensional accuracy and stability of DPA, indicated by decreased gap widths and discrepancies, support timely programmed tooth movement, emphasizing a force-driven mechanism beyond shape-driven behavior. However, sample heterogeneity, as indicated by large SD values, highlights the need to minimize factors that increase the gap width, including manufacturer-recommended insertion and removal techniques.

Several factors influence aligner force levels and gap width changes. The higher initial TFA forces may have resulted from the thicker (0.75 mm) PET-G sheets used in its fabrication [26, 27]. However, the thickness decreased to close to 0.5 mm according to a previous study [19], reaching DPA's thickness level. Although direct thickness comparisons were not performed, DPA demonstrated consistent thickness and dimensional accuracy across sets, unlike the site-specific thickness variations in TFA [7, 28]. Critically, the lowest thickness was on the facial surfaces of the central incisors, where the greatest force was exerted by the active TFA fit from vacuum compression. Thus, the dimensional accuracy with passive-fit adaptation may be more crucial than thickness differences. The vacuum thermal bonding process of TFA has limitations and requires adequate interproximal blocking to prevent patient discomfort. The shape memory properties of DPA eliminate this need, achieving a high fit even in intricate interproximal areas.

This study has some limitations. The sample size was small, particularly for micro-CT analysis, which limits the generalizability of the findings. Despite efforts to minimize these discrepancies, potential system errors may arise from force measurements using flat film sensors on curved tooth surfaces. The force range of the sensor was limited, necessitating the precise calibration of standardized measurements. As this was an *in vitro* study, it did not account for *in vivo* factors, such as saliva, occlusal forces, wearing time, and patient behavior, that could affect performance. Future *in vivo* studies with larger sample sizes are needed to enhance our understanding of DPA and overcome current clinical limitations.

## CONCLUSIONS

This study provides foundational evidence that DPAs deliver more stable and predictable orthodontic forces than TFAs, particularly under the conditions of repeated removal and varying dental crowding. These findings highlight the superior fit and dimensional stability of DPA, contributing to its consistent force application across different tooth positions and crowding scenarios. These advantages suggest that DPA can enhance treatment outcomes by reducing the risk of unexpected tooth movement regardless of the presence of

crowding. Despite these promising results, further *in vivo* studies with larger sample sizes are necessary to validate these findings and to fully understand the clinical applications of DPA. Additionally, addressing potential system errors and incorporating real-world factors are crucial for refining the efficacy of DPA and establishing it as a reliable alternative for orthodontic treatment.

## Abbreviations

3D, three-dimensional

C, crowding

CA, clear aligner

CT, computed tomography

DLP, digital light processing

DPA, direct-printed aligner

F, facial

FC, facial cusp

FG, faciogingival

IN, incisal

NC, non-crowding

OF, occlusal fossa

P, palatal

PC, palatal cusp

PET-G, polyethylene terephthalate glycol

PG, palatogingival

SD, standard deviation

STL, standard tessellation language

TFA, thermoformed aligner

UV, ultraviolet

## Declarations

## **Ethics approval and consent to participate**

Not applicable

## **Consent for publication**

Not applicable

## **Availability of data and material**

The datasets used and/or analyzed during the current study are available from the corresponding author on reasonable request.

## **Competing interests**

The authors declare that they have no competing interests.

## **Funding**

Not applicable

## **Authors' contributions**

ND and JC conducted experiments, analyzed the data, and were major contributors to writing the manuscript. KWP and HJ played supportive roles in micro-CT imaging. HK and JC interpreted the results based on the material properties of the aligners. SK designed the study. All authors read and approved the final manuscript.

## **Acknowledgements**

This work was supported by the Korea Medical Device Development Fund grant funded by the Korea government (the Ministry of Science and ICT, the Ministry of Trade, Industry and Energy, the Ministry of Health & Welfare, the Ministry of Food and Drug Safety). (Project Number: 2710001573, RS-2023-00223150)

## **References**

1. Gold BP, Siva S, Duraisamy S, Idaayath A, Kannan R. Properties of orthodontic clear aligner materials-a review. *J evol med dent sci*. 2021;10(37):3288-94.
2. Pacheco-Pereira C, Brandelli J, Flores-Mir C. Patient satisfaction and quality of life changes after Invisalign treatment. *Am J Orthod Dentofacial Orthop*. 2018;153(6):834-41.
3. Zhang B, Huang X, Huo S, Zhang C, Zhao S, Cen X, et al. Effect of clear aligners on oral health-related quality of life: A systematic review. *Orthod Craniofac Res*. 2020;23(4):363-70.
4. Ghislanzoni LH, Kalemaj Z, Manuelli M, Magni C, Polimeni A, Lucchese A. How well does Invisalign ClinCheck predict actual results: A prospective study. *Orthod Craniofac Res*. 2024;27(3):465-73.
5. Papadimitriou A, Mousoulea S, Gkantidis N, Kloukos D. Clinical effectiveness of Invisalign(R) orthodontic treatment: a systematic review. *Prog Orthod*. 2018;19(1):37.



6. Robertson L, Kaur H, Fagundes NCF, Romanyk D, Major P, Flores Mir C. Effectiveness of clear aligner therapy for orthodontic treatment: A systematic review. *Orthod Craniofac Res.* 2020;23(2):133-42.
7. Jindal P, Juneja M, Siena FL, Bajaj D, Breedon P. Mechanical and geometric properties of thermoformed and 3D printed clear dental aligners. *Am J Orthod Dentofacial Orthop.* 2019;156(5):694-701.
8. Can E, Panayi N, Polychronis G, Papageorgiou SN, Zinelis S, Eliades G, et al. In-house 3D-printed aligners: effect of in vivo ageing on mechanical properties. *Eur J Orthod.* 2022;44(1):51-5.
9. Lee SY, Kim H, Kim HJ, Chung CJ, Choi YJ, Kim SJ, et al. Thermo-mechanical properties of 3D printed photocurable shape memory resin for clear aligners. *Sci Rep.* 2022;12(1):6246.
10. Pratsinis H, Papageorgiou SN, Panayi N, Iliadi A, Eliades T, Kletsas D. Cytotoxicity and estrogenicity of a novel 3-dimensional printed orthodontic aligner. *Am J Orthod Dentofacial Orthop.* 2022;162(3):e116-e22.
11. Hertan E, McCray J, Bankhead B, Kim KB. Force profile assessment of direct-printed aligners versus thermoformed aligners and the effects of non-engaged surface patterns. *Prog Orthod.* 2022;23(1):49.
12. Schupp W, Haubrich J, Klingberg M, Boisserée W, Sim U-s, Kim H. Shape memory aligners: a new dimension in aligner orthodontics. *Journal of Aligner Orthodontics.* 2023;7(2):113-27.
13. Grant J, Foley P, Bankhead B, Miranda G, Adel SM, Kim KB. Forces and moments generated by 3D direct printed clear aligners of varying labial and lingual thicknesses during lingual movement of maxillary central incisor: an in vitro study. *Prog Orthod.* 2023;24(1):23.
14. McKay A, McCray J, Bankhead B, Lee MM, Miranda G, Adel SM, et al. Forces and moments generated during extrusion of a maxillary central incisor with clear aligners: an in vitro study. *BMC Oral Health.* 2023;23(1):495.
15. Sharif M, Bourauel C, Ghoneima A, Schwarze J, Alhotan A, Elshazly TM. Force system of 3D-printed orthodontic aligners made of shape memory polymers: an in vitro study. *Virtual and Physical Prototyping.* 2024;19(1):e2361857.
16. Manoukakis T, Nikolaidis AK, Koulaouzidou EA. Polymerization kinetics of 3D-printed orthodontic aligners under different UV post-curing conditions. *Prog Orthod.* 2024;25(1):42.
17. Lombardo L, Palone M, Longo M, Arveda N, Nacucchi M, De Pascalis F, et al. MicroCT X-ray comparison of aligner gap and thickness of six brands of aligners: an in-vitro study. *Prog Orthod.* 2020;21(1):12.
18. Koenig N, Choi JY, McCray J, Hayes A, Schneider P, Kim KB. Comparison of dimensional accuracy between direct-printed and thermoformed aligners. *Korean J Orthod.* 2022;52(4):249-57.
19. Park SY, Choi SH, Yu HS, Kim SJ, Kim H, Kim KB, et al. Comparison of translucency, thickness, and gap width of thermoformed and 3D-printed clear aligners using micro-CT and spectrophotometer. *Sci Rep.* 2023;13(1):10921.
20. Skaik A, Wei XL, Abusamak I, Iddi I. Effects of time and clear aligner removal frequency on the force delivered by different polyethylene terephthalate glycol-modified materials determined with thin-film pressure sensors. *Am J Orthod Dentofacial Orthop.* 2019;155(1):98-107.
21. Upadhyay M, Arqub SA. Biomechanics of clear aligners: hidden truths & first principles. *Journal of the World Federation of Orthodontists.* 2022;11(1):12-21.
22. Elkholy F, Schmidt S, Schmidt F, Amirkhani M, Lapatki BG. Force decay of polyethylene terephthalate glycol aligner materials during simulation of typical clinical loading/unloading scenarios. *J Orofac*

Orthop. 2023;84(3):189-201.

23. Lombardo L, Martines E, Mazzanti V, Arreghini A, Mollica F, Siciliani G. Stress relaxation properties of four orthodontic aligner materials: A 24-hour in vitro study. *Angle Orthod.* 2017;87(1):11-8.
24. Fiori A, Minervini G, Nucci L, d'Apuzzo F, Perillo L, Grassia V. Predictability of crowding resolution in clear aligner treatment. *Prog Orthod.* 2022;23(1):43.
25. Linjawi AI, Abushal AM. Adaptational changes in clear aligner fit with time. *Angle Orthod.* 2022;92(2):220-5.
26. Hahn W, Dathe H, Fialka-Fricke J, Fricke-Zech S, Zapf A, Kubein-Meesenburg D, et al. Influence of thermoplastic appliance thickness on the magnitude of force delivered to a maxillary central incisor during tipping. *Am J Orthod Dentofacial Orthop.* 2009;136(1):12 e1-7; discussion -3.
27. Bucci R, Rongo R, Levate C, Michelotti A, Barone S, Razionale AV, et al. Thickness of orthodontic clear aligners after thermoforming and after 10 days of intraoral exposure: a prospective clinical study. *Prog Orthod.* 2019;20(1):36.
28. Tartaglia GM, Mapelli A, Maspero C, Santaniello T, Serafin M, Farronato M, et al. Direct 3D Printing of Clear Orthodontic Aligners: Current State and Future Possibilities. *Materials (Basel).* 2021;14(7).

## Figures

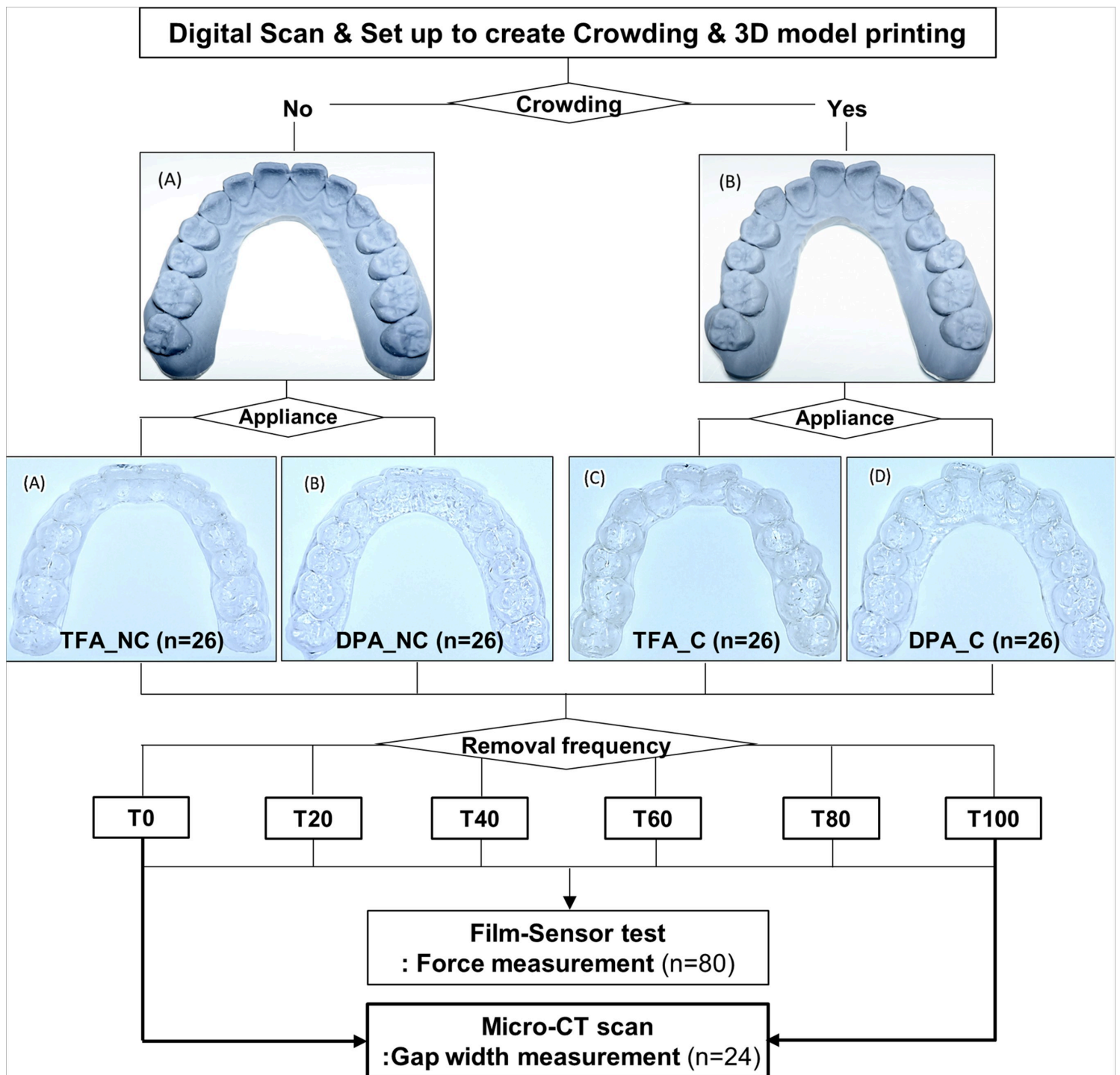


**Figure 1**

Diagrammatic flowchart of experimental design.

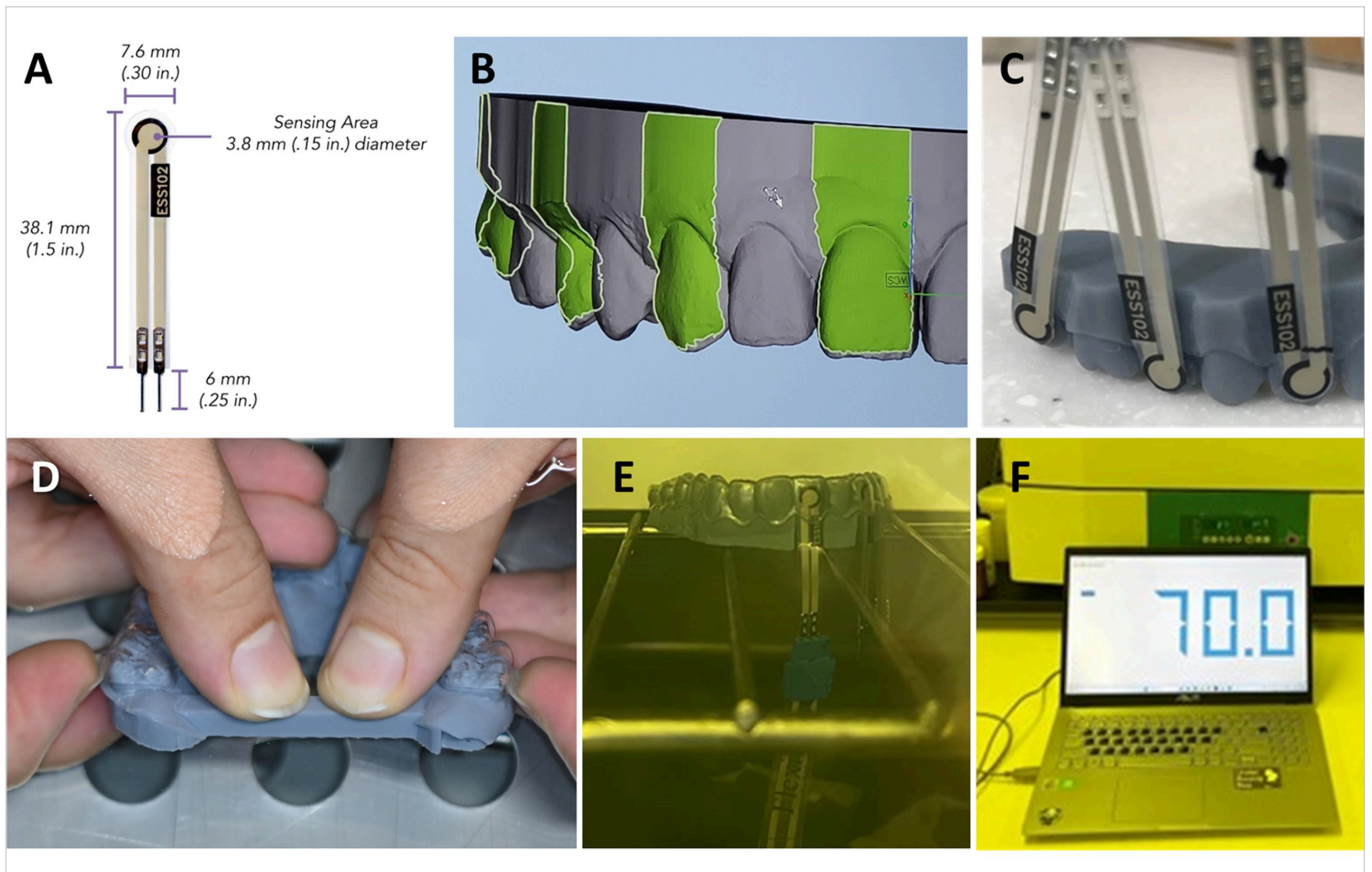


**Figure 2**

Force measurement process. (A) FlexiForce ESS102 sensors used for measuring forces. (B) Digital surface design of the printed model, providing space for sensor placement to ensure the best passive fit of the aligner. (C) Sensors attached to the tested teeth surfaces of the printed model. (D) Repeated aligner insertion and removal procedure conducted on the master model in a water bath at 40°C. (E, F) Data collection of force measurements with aligner seated on the prepared model within an oven set at 37°C.

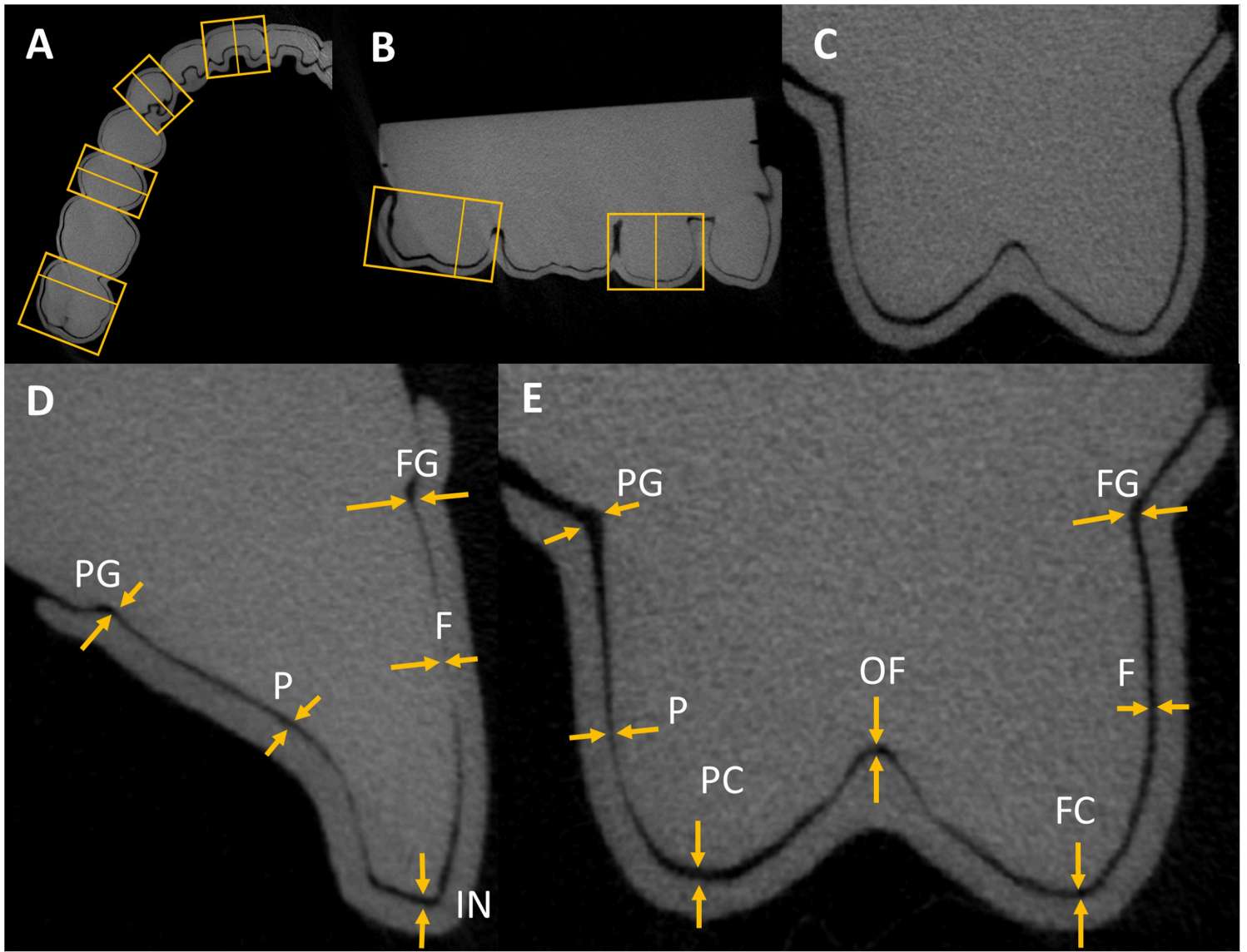


**Figure 3**

Micro-CTs illustrating the gap width between aligners and teeth at reference points. (A) Axial view showing the region settings for each tooth. (B) Sagittal view showing the region settings for each tooth. (C) Micro-CT cross-sectional images of the designated region. (D) Anterior teeth (e.g., the central incisor). (E) Posterior teeth (e.g., the second premolar). Yellow arrows indicate the reference points on the teeth.



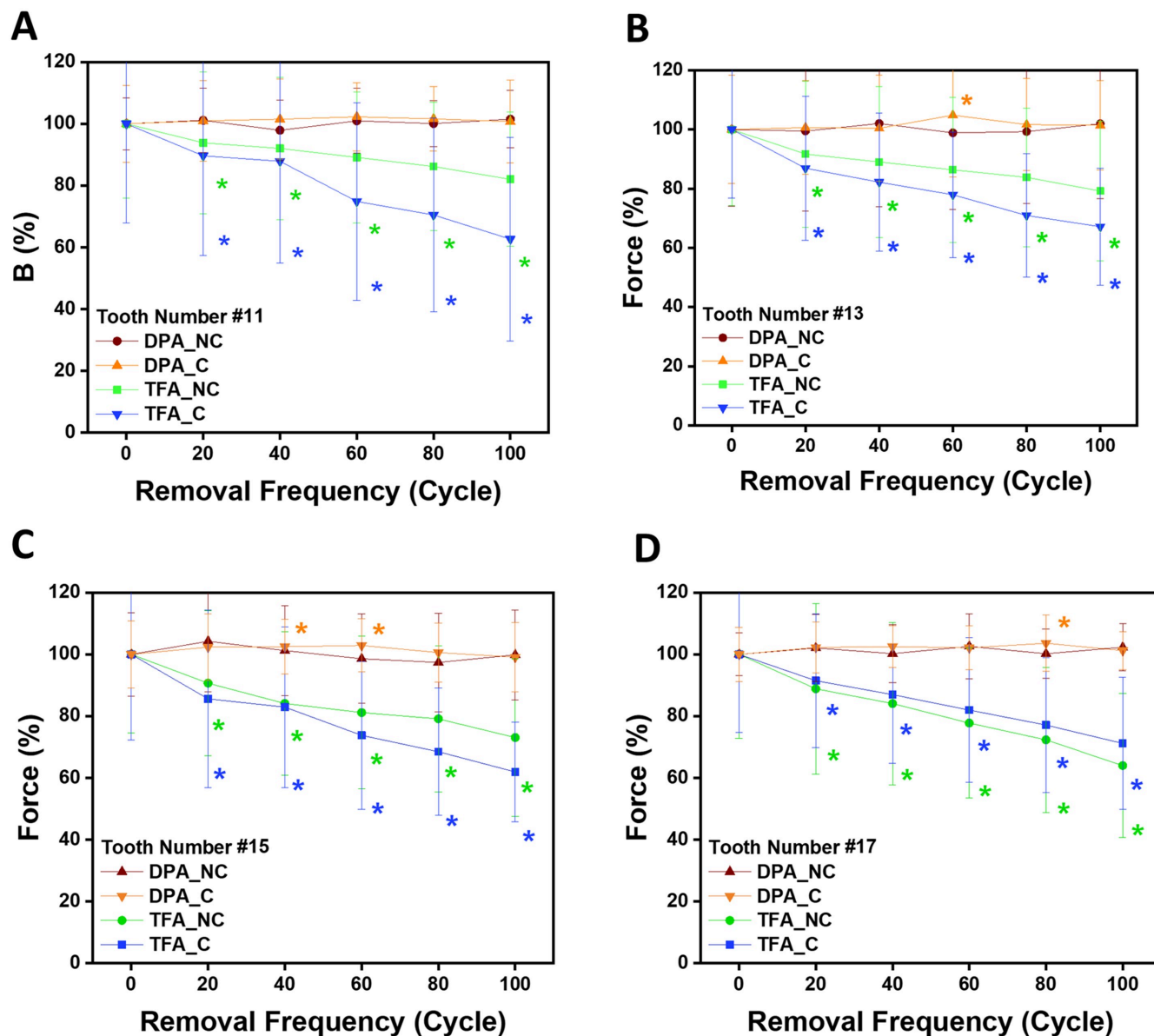


**Figure 4**

Changes in force delivery of direct-printed and thermoformed clear aligners over removal frequency, expressed as a percentage. The initial force delivery is set to 100%, illustrating the relative changes in force as removal frequency increases. The panels show changes for different teeth: (A) Tooth #11, (B) Tooth #13, (C) Tooth #15, and (D) Tooth #17.

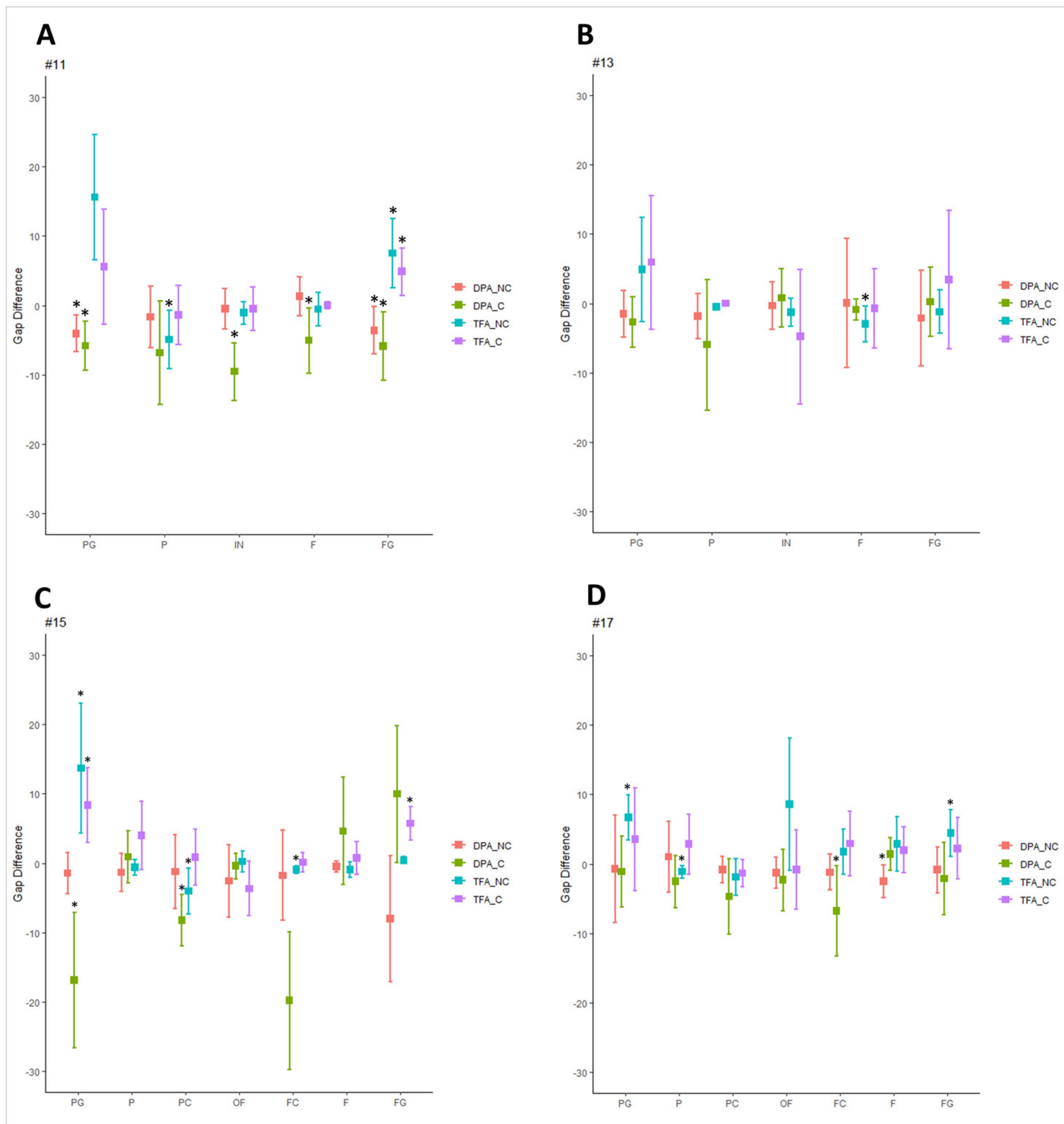


**Figure 5**

The differences in gap width between the model and aligner after 100 removal cycles, comparing direct-printed and thermoformed clear aligners across various tooth regions in both crowding and non-crowding groups. The panels show changes for different teeth: (A) Tooth #11, (B) Tooth #13, (C) Tooth #15, and (D) Tooth #17.